DOI: 10.1021/ma902143g

Macromolecules
ARTICLE

Hierarchically Ordered Microstructures Self-Assembled from $A(BC)_n$ Multiblock Copolymers

Liquan Wang, Jiaping Lin,* and Liangshun Zhang

Shanghai Key Laboratory of Advanced Polymeric Materials, Key Laboratory for Ultrafine Materials of Ministry of Education, School of Materials Science and Engineering, East China University of Science and Technology, Shanghai 200237, China

Received September 27, 2009; Revised Manuscript Received December 21, 2009

ABSTRACT: Using real-space self-consistent field theory, we explored hierarchical microstructures self-assembled from $A(BC)_n$ multiblock copolymers. The multiblock copolymers were classified into two types in terms of relative magnitude of A/B and A/C interaction strengths: one is that $\chi_{AB}N$ is less than or equal to $\chi_{AC}N$, and the other is that $\chi_{AB}N$ is greater than $\chi_{AC}N$. For both cases, the multiblock copolymers can self-assemble into hierarchically ordered microstructures with two different length scales. For $\chi_{AB}N \leq \chi_{AC}N$, various hierarchical microstructures, such as cylinders-in-lamellae$^{\|}$, lamellae-in-lamella$^{\|}$, cylinders-in-cylinder$^{\|}$, and spheres-in-sphere$^{\|}$, were observed. In these microphases, the small-length-scale structures and the large-length-scale structures are packed in the doubly parallel forms. It was found the number of internal small-length-scale structures can be tailored by tuning the number of BC block and the interaction strength between A and BC blocks. For $\chi_{AB}N > \chi_{AC}N$, in addition to the parallel packed hierarchical structures, the multiblock copolymers can self-organize into perpendicular packed hierarchical structures, in which the structures with small periods are arranged perpendicular to structures with large periods. These perpendicular packed hierarchical structures were found to be only stable at higher value of $\chi_{BC}N$.

Introduction

Nanostructured materials, created by spontaneous self-assembly of building molecules, have attracted much attention for their diversiform nanoscale structure as well as promising potential properties.[1−5] With the process of macromolecule chemistry, a variety of building molecules including linear copolymers and nonlinear copolymers have been prepared for designing functional materials. Among these building molecules, block copolymers serve as one promising class for nanotechnology. Usually, simple (e.g., AB or ABA) block copolymers exhibit a single periodic nanostructure that depends on the molecular architecture and characteristic.[6−12] However, by designing molecules with more complicated architectures (e.g., ABC triblock copolymer),[13−16] block copolymers may generate hierarchical self-assembled microstructures, which possess several periodicities like noncentrosymmetric superlattices.[17] The possibility of forming hierarchical structure from block copolymers could bring a significant advance in applications requiring materials built with multiple-length-scale structures, such as photonic crystals.[18]

The hierarchical structures involving multiple length scales have been found in block copolymers with special building architectures. For example, ten Brinke and co-workers observed a series of structure-in-structure morphologies self-assembled from a supramolecular comb−coil block copolymer which consists of diblock copolymers with low molecular weight compound linked to the block copolymer chains.[19−26] The hierarchical structures are reported to possess double periodicities, including the large period of diblock copolymers and the small period of comb-shaped blocks. An alternative molecular architecture for creating hierarchical structures is a linear multiblock copolymer, which is comprised of one or two tails and many midblocks.[27−33] In such a system, the large-length-scale period is related to the microphase separation between tails and midblocks, while the small-length-scale period is involved in the segregation within midblocks. The ability of linear multiblock copolymers to form hierarchical structures has been demonstrated in recent experimental studies. Matsushita et al. reported various fully parallel structure-in-structures, such as onionlike sphere and coaxial cylinder, from the self-assembly of $V(IS)_nIV$ and $V(IS)_nI$ multiblock copolymers, where V, I, and S refer to poly(2-vinylpyridine), polyisoprene, and polystyrene, respectively.[27−31] They found that the lengths of V blocks and the number of IS midblock can influence the ordered phases at large length scale and the amount of substructures, respectively. Further studies by Bates et al. showed that the arrangement of substructures relative to large structures can also be tuned by changing the molecular nature.[32,33] They prepared a CECECP hexablock copolymer containing a long poly(ethylene-*alt*-polylene) (P) tail block and five short polycyclohexylethylene (C) and polyethylene (E) middle blocks. Because of the exceptional sequence of interaction parameters, the CECECP hexablock copolymer microphase separated into novel perpendicular lamellae in parallel lamellae structures that contain strips of C and E forming layers arranged normal to alternating lamella formed by P. Inspiringly, the window of hierarchical structures has been greatly expanded by virtue of updating the molecular architectures and characteristic. However, because of the diversity and complexity of the structure-in-structures, the phase behavior has yet to be further developed.

Apart from the experimental investigations, simulations as well as theories that can provide molecular level insights for understanding the hierarchical phase behavior of complex block copolymers have been applied.[34−39] For example, the theories and simulations such as a strong segregation theory and dissipative particle dynamic simulations have accounted for the self-assembly of $A(BA)_nBA$ and $A(BC)_nBA$ multiblock copolymers.[34−37]

*Corresponding author: Tel +86-21-64253370; Fax +86-21-64253539; e-mail jlin@ecust.edu.cn, jplinlab@online.sh.cn.

 Published on Web 01/14/2010

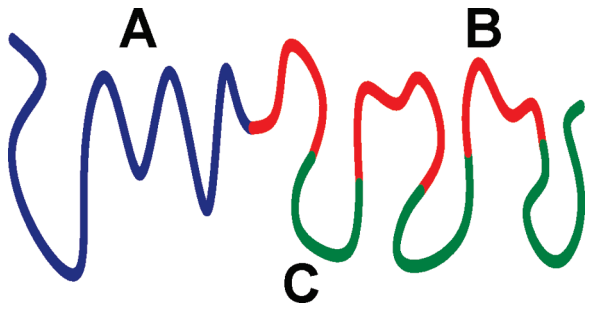

Figure 1. Schematic representation of $A(BC)_n$ multiblock copolymer with $n = 3$.

So far, a widely used theory for predicting equilibrium mesophase structures of polymers is the self-consistent field theory (SCFT).[40−57] ten Brinke et al. first extended the SCFT to investigate the $A(BA)_n$ multiblock copolymers consisting of a long A block connected to a $(BA)_n$ multiblock.[38] It is demonstrated that hierarchical lamellar structure with two different length scales is formed. The method was also used to conduct a more comprehensive investigation of the formation of hierarchical lamellae in $A(BC)_nBA$ multiblock copolymers by Li et al.[39] Phase diagrams were constructed to illustrate the relationship between hierarchical lamellae and molecular characteristics. However, for the theoretical studies of multiblock copolymers, recent efforts were only limited to the lamellae-in-lamella structures with parallel arrangement of two different-length-scale structures. For further exploring more complicated structures, one major obstacle is the accurate solution of SCFT diffusion equation. Recently, Fredrickson proposed a fourth-order backward differentiation formula (BDF4) for solving diffusion equation, which has higher accuracy and stability for strongly segregated systems.[58] By means of this method, more complicated hierarchical structures, which appear at higher interaction strength, may be observed.[59] Relying on the superiority of the BDF4 method, we take advantage of SCFT to undertake a systematical investigation on the hierarchical phase behavior of multiblock copolymers owing to the lack of comprehensive theoretical studies.

In the present work, the real-space SCFT combined with BDF4 method was applied for the study of multiblock copolymers with the architecture of $A(BC)_n$ style. In addition to the parallel packed hierarchical structures, we found theoretically, for the first time, that $A(BC)_n$ multiblock copolymers can self-assemble into perpendicular packed hierarchical structures. Novel perpendicular packed hierarchical structures, such as lamellae-in-cylinder$^{\perp}$ and lamellae-in-sphere$^{\perp}$, were predicted. Among them, the structures of perpendicular packed lamellae-in-lamella are confirmed by latest experimental results.[32,33] For the parallel packed hierarchical structures, the number of internal BC substructures can be controlled by change of n value and $\chi_{AB}N$ (or $\chi_{AC}N$). Moreover, the perpendicular packed hierarchical structures only emerge when the $\chi_{BC}N$ value is higher at $\chi_{AB}N > \chi_{AC}N$. We expect that the present study may provide a rational understanding of the doubly periodic microstructures with different arrangements.

Theoretical Method

We consider a system with volume V containing $A(BC)_n$ multiblock copolymers. Each copolymer consists of an A end block connected to a $(BC)_n$ multiblock composed of n elementary diblock repeat units, as schematically illustrated in Figure 1. The copolymers are assumed to be monodisperse. The volume fractions of A, B, and C blocks are f_A, f_B, and f_C, respectively. The total degree of polymerization of the multiblock copolymer is N, and the total lengths of A, B, and C blocks are f_AN, f_BN, and f_CN, respectively. The B blocks and C blocks are assumed to be equal, and the volume fractions of B block and C block are specified by $\Delta f_B = \Delta f_C = (1 - f_A)/2n$.

In the SCFT model, one considers the configurations of a single copolymer chain in a set of effective chemical potential field $\omega_I(\mathbf{r})$, where I denotes block species A, B, and C. We invoke an incompressibility ($\varphi_A(\mathbf{r}) + \varphi_B(\mathbf{r}) + \varphi_C(\mathbf{r}) = 1$) by introducing a Lagrange multiplier $\xi(\mathbf{r})$. The free energy per chain is given by

$$\frac{F}{nk_BT} = -\ln\left(\frac{Q}{V}\right) + \frac{1}{V}\int d\mathbf{r}\{ \sum_{\substack{I,J = A,B,C \\ I \neq J}} \chi_{IJ}N\varphi_I(\mathbf{r})\varphi_J(\mathbf{r}) - \sum_{I=A,B,C} \omega_I(\mathbf{r})\varphi_I(\mathbf{r}) - \xi(\mathbf{r})(1 - \sum_{I=A,B,C} \varphi_I(\mathbf{r}))\} \quad (1)$$

where χ_{IJ} is the Flory−Huggins parameter between different species I and J. Q is the partition function of a single chain in the effective chemical potential field $\omega_I(\mathbf{r})$ (I = A, B, C) in terms of propagators $q(\mathbf{r},s)$ and $q^+(\mathbf{r},s)$. The spatial coordinate $\mathbf{r}$ is rescaled by R_g, where ${R_g}^2 = a^2N/6$. The contour length is parametrized with variable s, which starts from one end ($s = 0$) to the other ($s = 1$). The propagators $q(\mathbf{r},s)$ and $q^+(\mathbf{r},s)$ satisfy following modified diffusion equations:

$$\frac{\partial q(r,s)}{\partial s} = [{R_g}^2\nabla^2 - \omega_{\theta(s)}(r)]q(r,s)$$
$$-\frac{\partial q^+(r,s)}{\partial s} = [{R_g}^2\nabla^2 - \omega_{\theta(s)}(r)]q^+(r,s) \quad (2)$$

with the initial condition $q(\mathbf{r},0) = 1$ and $q^+(\mathbf{r},0) = 1$, respectively. Here, $\theta(s)$ is used to specify the segment type along the copolymer chain, subject to ($0 \le i < n$)

$$\theta(s) = \begin{cases} A \text{ if } 0 < s < f_A \\ B \text{ if } f_A + i(\Delta f_B + \Delta f_C) < s < f_A + i(\Delta f_B + \Delta f_C) + \Delta f_B \\ C \text{ if } f_A + i(\Delta f_B + \Delta f_C) + \Delta f_B < s < f_A + (i+1)(\Delta f_B + \Delta f_C) \end{cases} \quad (3)$$

The product of $q(\mathbf{r},s)q^+(\mathbf{r},s)$ provides the partition function for a molecule with its sth segment constrained to positions $\mathbf{r}$. The partition function, Q, for an unconstrained chain is evaluated by summing over all possible position $\mathbf{r}$ of the sth segment, given by $Q = \int d\mathbf{r}\ q(\mathbf{r},s)q^+(\mathbf{r},s)$. The integral is independent of s. Furthermore, the product of $q(\mathbf{r},s)q^+(\mathbf{r},s)$ is proportional to the distribution of the sth segment. From the fact that the volume average of each block must equal to the volume fraction of corresponding block, the segment densities $\varphi_A(\mathbf{r})$, $\varphi_B(\mathbf{r})$, and $\varphi_C(\mathbf{r})$ follow that

$$\varphi_A(\mathbf{r}) = \frac{V}{Q}\int_0^{f_A} ds\ q(\mathbf{r},s)q^+(\mathbf{r},s) \quad (4)$$

$$\varphi_B(\mathbf{r}) = \frac{V}{Q}\sum_{i=0}^{n-1}\int_{f_A + i(\Delta f_B + \Delta f_C)}^{f_A + i(\Delta f_B + \Delta f_C) + \Delta f_B} ds\ q(\mathbf{r},s)q^+(\mathbf{r},s) \quad (5)$$

$$\varphi_C(\mathbf{r}) = \frac{V}{Q}\sum_{i=0}^{n-1}\int_{f_A + i(\Delta f_B + \Delta f_C) + \Delta f_B}^{f_A + (i+1)(\Delta f_B + \Delta f_C)} ds\ q(\mathbf{r},s)q^+(\mathbf{r},s) \quad (6)$$

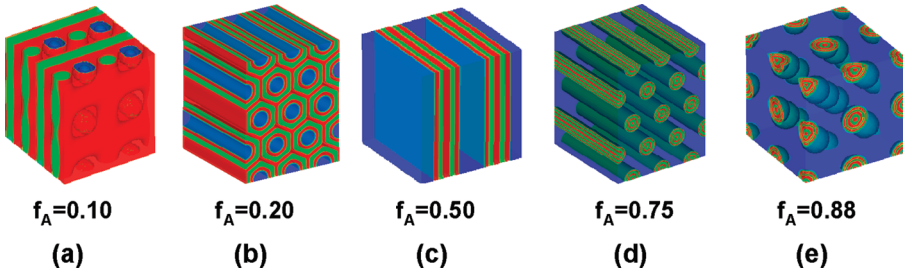

Figure 2. Hierarchical microstructures self-assembled from A(BC)$_3$ multiblock copolymer with $\chi_{AB}N = 200$, $\chi_{AC}N = 250$, and $\chi_{BC}N = 500$: (a) spheres-in-lamellae$^{\|}$, (b) cylinders-in-lamellae$^{\|}$, (c) lamellae-in-lamella$^{\|}$, (d) cylinders-in-cylinder$^{\|}$, and (e) spheres-in-sphere$^{\|}$. From (a) to (e), the volume fractions of A blocks are 0.10, 0.20, 0.50, 0.75, and 0.88, respectively. The blue, red, and green colors are assigned to A, B, and C blocks, respectively.

Minimization of free energy F, with respect to $\varphi_A(\mathbf{r})$, $\varphi_B(\mathbf{r})$, $\varphi_C(\mathbf{r})$, and $\xi(\mathbf{r})$, can lead to a set of mean-field equations:

$$\omega_A(\mathbf{r}) = \chi_{AB}N\varphi_B(\mathbf{r}) + \chi_{AC}N\varphi_C(\mathbf{r}) + \xi(\mathbf{r}) \quad (7)$$

$$\omega_B(\mathbf{r}) = \chi_{AB}N\varphi_A(\mathbf{r}) + \chi_{BC}N\varphi_C(\mathbf{r}) + \xi(\mathbf{r}) \quad (8)$$

$$\omega_C(\mathbf{r}) = \chi_{AC}N\varphi_A(\mathbf{r}) + \chi_{BC}N\varphi_B(\mathbf{r}) + \xi(\mathbf{r}) \quad (9)$$

$$\varphi_A(\mathbf{r}) + \varphi_B(\mathbf{r}) + \varphi_C(\mathbf{r}) = 1 \quad (10)$$

The free energy (in units of k_BT) can be decomposed into[60]

$$F = U - TS \quad (11)$$

Here, U and S are the internal energy contribution and conformational entropy contribution to free energy, respectively. These quantities are given by

$$U = \frac{\chi_{AB}N}{V}\int d\mathbf{r}\ \varphi_A(\mathbf{r})\varphi_B(\mathbf{r}) + \frac{\chi_{BC}N}{V}\int d\mathbf{r}\ \varphi_B(\mathbf{r})\varphi_C(\mathbf{r}) + \frac{\chi_{AC}N}{V}\int d\mathbf{r}\ \varphi_A(\mathbf{r})\varphi_C(\mathbf{r}) \quad (12)$$

$$-TS = -\ln\left(\frac{Q}{V}\right) - \frac{1}{V}\int d\mathbf{r}\ [\omega_A(\mathbf{r})\varphi_A(\mathbf{r}) + \omega_B(\mathbf{r})\varphi_B(\mathbf{r}) + \omega_C(\mathbf{r})\varphi_C(\mathbf{r})] \quad (13)$$

To solve the SCFT equations, we use a variant of the algorithm developed by Fredrickson and co-workers.[40−43] The calculations were started from a random initial state. The diffusion equations were solved with the fourth-order backward differentiation formula (BDF4), which has higher accuracy and stability for strongly segregated systems.[58,61] For example, the diffusion equation, eq 2, is discretized according to

$$\frac{25}{12}q_{n+1} - 4q_n + 3q_{n-1} - \frac{4}{3}q_{n-2} + \frac{1}{4}q_{n-3} = \Delta s R_g^2\nabla^2 q_{n+1} - \Delta s\omega_{\theta(s)}(4q_n - 6q_{n-1} + 4q_{n-2} - q_{n-3}) \quad (14)$$

In this expression, q_{n+i} denotes $q(\mathbf{r},(n+i)\Delta s)$, and Δs is the step size. The initial values required to apply this formula are obtained by using backward Euler and Richardson's extrapolation. The densities $\phi_I(\mathbf{r})$ of special I, conjugated the chemical potential fields $\omega_I(\mathbf{r})$, are evaluated with respective to eqs 4−9. The chemical potential fields $\omega_I(\mathbf{r})$ can be updated by using a two-step Anderson mixing scheme.[62]

The simulations in this work were carried out in three-dimensions with periodic boundary conditions. In the calculations, the spatial resolutions were taken as $\Delta x < 0.15R_g$. We tested several contour step sizes at higher interaction strength. It was found that the free energy can converge to a stable value when contour step size is smaller than about 0.0015. Thus, the contour step sizes in the simulation were set at $\Delta s = 0.001$, which is sufficient to guarantee the accuracy. The numerical simulations proceeded until the relative free energy changes at each iteration were smaller than 10^{-6} and the incompressibility condition was achieved. We optimized the free energy with respect to the size of simulation box, as suggested by Bohbot-Raviv and Wang.[63] In the optimization, the free energies were found to have many local minima, corresponding to hierarchical microstructures with different number of substructures. The stable microstructure was obtained until the global minimum of free energy was achieved.

Results and Discussion

In this work, we investigate the case that the volume fractions of B block and C block are equal ($\Delta f_B = \Delta f_C$). Experimental observations of the self-assembly of this kind of multiblock copolymers are reported in the literature.[27−33] We classify the multiblock copolymer melts into two categories according to the relative magnitude of interaction strength $\chi_{AB}N$ compared to $\chi_{AC}N$. One is that $\chi_{AB}N \le \chi_{AC}N$, and the other is that $\chi_{AB}N > \chi_{AC}N$. These two types are distinguished by the relative cost between A/B and A/C interfacial contacts. The A/B interfaces are imposed by the connectivity of molecular architectures, whereas the A/C interfaces form only when they are energetically favored.

1. A(BC)$_n$ Multiblock Copolymers with $\chi_{AB}N \le \chi_{AC}N$. For this case, the interaction strength $\chi_{AB}N$ was set to be less than or equal to $\chi_{AC}N$. Furthermore, the $\chi_{BC}N$ was chosen to be strong enough to ensure the appearance of hierarchical microstructures. Under this circumstance, the interactions between the A blocks and B blocks are less thermodynamically costly than those of A blocks and C blocks, which is unfavorable for the A/C interface to be produced.[64]

We first consider the model of A(BC)$_n$ multiblock copolymers with $n = 3$ at $\chi_{AB}N = 200$, $\chi_{AC}N = 250$, and $\chi_{BC}N = 500$. Figure 2 shows the hierarchically ordered structures observed at various volume fractions f_A of A blocks. As can be seen from Figure 2a, the A(BC)$_n$ multiblock copolymers form a spheres-in-lamellae$^{\|}$ structure (prime symbol $\|$ denotes the two length-scale-order structures are in parallel) when A volume fraction is lower ($f_A = 0.10$). In the microstructure, the spheres formed by A blocks are surrounded by alternating BC lamellae as a matrix. When f_A increases to 0.20, the multiblock copolymers self-assemble into the cylinders-in-lamellae$^{\|}$ structure where the cylinders of A blocks are hexagonally aligned in the matrix of five-layered BC lamellae (see Figure 2b). When f_A value is 0.50, a

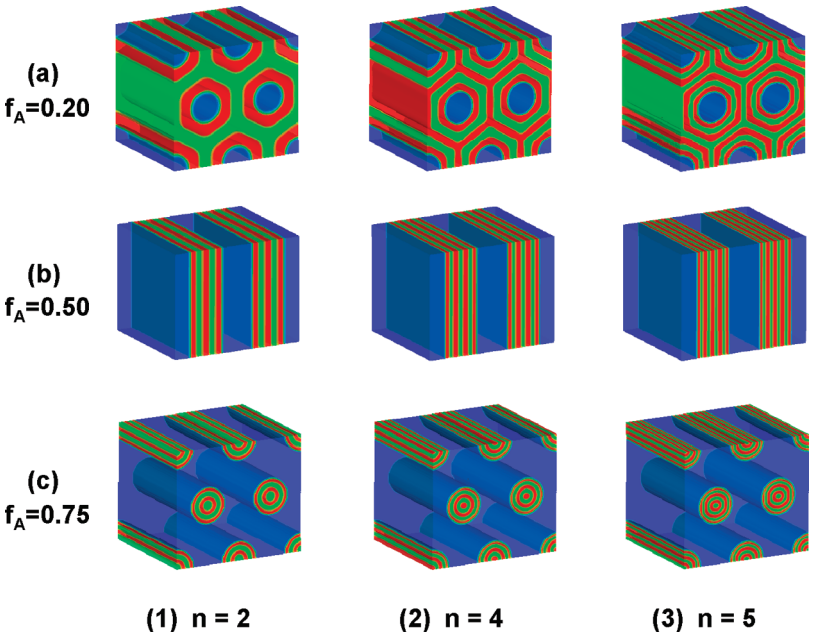

Figure 3. Hierarchical microstructures of (a) cylinders-in-lamellae[‖] (f_A = 0.20), (b) lamellae-in-lamella[‖] (f_A = 0.50), and (c) cylinders-in-cylinder[‖] (f_A = 0.75) for $A(BC)_n$ multiblock copolymer with various number n of repeating BC blocks: (1) n = 2, (2) n = 4, and (3) n = 5. The average interaction parameters are $\chi_{AB}N/n$ = 40, $\chi_{AC}N/n$ = 45, and $\chi_{BC}N/n$ = 40. The blue, red, and green colors are assigned to A, B, and C blocks, respectively.

lamellae-in-lamella[‖] is observed, which contains one thick A lamella and five thin BCBCB lamellae. At higher value of A volume fraction, the A blocks form the matrix while B and C blocks form the minority domain. As shown in Figure 2d (f_A = 0.75), the B and C blocks are segregated into concentric cylinders hexagonally dispersed in the matrix from A blocks. Figure 2e shows cubic-centered spheres where B and C blocks are separated concentrically into BCBCB spheres at f_A = 0.88. We refer to the microstructures shown in parts d and e of Figure 2 as cylinders-in-cylinder[‖] and spheres-in-sphere[‖], respectively.

It is apparent from Figure 2 that the hierarchical microstructures are composed of multiply internal BC substructures. Further studies revealed that the number of internal BC substructures is dependent on the number n of repeating BC blocks. Figure 3 shows the hierarchical microstructures at various n values. The average interaction strength $\chi N/n$ is used to account properly for the effect of changing n and exclude the influence of variation of segment−segment interaction strength. The interaction parameters in Figure 3 are $\chi_{AB}N/n$ = 40, $\chi_{AC}N/n$ = 45, and $\chi_{BC}N/n$ = 40. Three kinds of hierarchical structures are shown as examples, including cylinders-in-lamellae[‖], lamellae-in-lamella[‖], and cylinders-in-cylinder[‖]. For cylinders-in-lamellae[‖] structure at f_A = 0.20 (Figure 3a), as the value of n increases from 2 to 4 and then to 5, the matrix of B and C is split into three layers, five layers, and seven layers, respectively. For lamellae-in-lamella[‖] at f_A = 0.50 (Figure 3b), the number of internal BC layers is 5, 7, and 9 for n = 2, 4, and 5, respectively. For cylinders-in-cylinder[‖] at f_A = 0.75 (Figure 3c), when the n value is equal to 2, 4, and 5, the number of concentric subcylinders is 4, 5, and 6, respectively.

In addition to n, the interaction strength also has an effect on the number of internal BC substructures. We plotted the free energy difference of lamellae-in-lamella[‖] between nine layers and seven layers for $A(BC)_5$ multiblock copolymer with $\chi_{BC}N$ = 200 and f_A = 0.5, which is presented in Figure 4a. In the calculations, the interaction parameter $\chi_{AB}N$ is set to be equal to $\chi_{AC}N$ and the $\chi_{AB/C}N$ is used to represent $\chi_{AB}N$ or $\chi_{AC}N$. When $\chi_{AB/C}N$ is smaller,

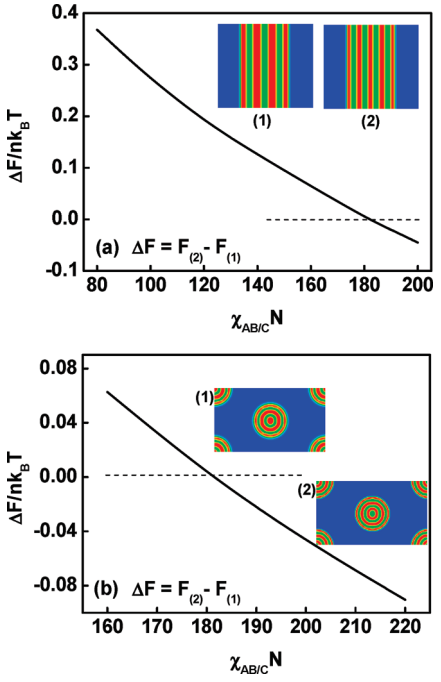

Figure 4. Free energy difference for different hierarchical structures of $A(BC)_5$ multiblock copolymers: (a) lamellae-in-lamella[‖] (f_A = 0.50 and $\chi_{BC}N$ = 200) and (b) cylinders-in-cylinder[‖] (f_A = 0.75 and $\chi_{BC}N$ = 400). The insets (1) and (2) show the hierarchical structures with different number of small-length-scale structures. ΔF is the difference of free energy between structures (2) and (1), i.e., $\Delta F = F_{(2)} - F_{(1)}$.

the lamellae-in-lamella[‖] with seven layers is stable. As $\chi_{AB/C}N$ increases, the difference of free energy decreases. When $\chi_{AB/C}N$ increases to 180, the free energy difference becomes negative, implying that the lamellae-in-lamella[‖] with nine layers becomes stable instead of that with seven layers. In addition, the $\chi_{AB/C}N$ also plays a role in determining internal BC substructure number of other structures, such as cylinders-in-cylinder[‖]. Figure 4b shows the free energy difference for $A(BC)_5$ multiblock copolymer with $\chi_{BC}N$ = 400 and

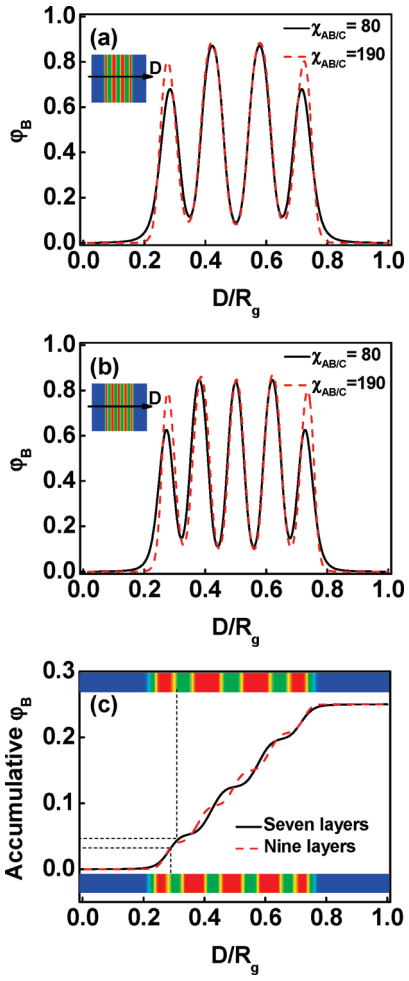

Figure 5. Density profile of B blocks on a cross section of lamellae-in-lamella marked by an arrow in the inset at $n = 5$, $f_A = 0.50$, and $\chi_{BC}N = 200$: (a) lamellae-in-lamella$^{\|}$ with seven layers and (b) lamellae-in-lamella$^{\|}$ with nine layers. The inserts in (a) and (b) show the lamellae-in-lamella$^{\|}$ structure with different small layers. The (c) shows the accumulative density of B blocks for the stable lamellae-in-lamella$^{\|}$ structure at $\chi_{AB/C}N = 80$ and $\chi_{AB/C}N = 190$. The dotted lines were drawn to indicate the accumulate density of outer layers of hierarchical lamella.

$f_A = 0.75$. The cylinders-in-cylinder$^{\|}$ with five concentric cylinders appears when $\chi_{AB/C}N$ is less than 182, while the cylinders-in-cylinder$^{\|}$ with six concentric cylinders emerges when $\chi_{AB/C}N$ is greater than 182.

To further clarify the dependence of the number of thin substructures on the $\chi_{AB/C}N$ value, the density profile of B blocks was plotted for the lamellae-in-lamella$^{\|}$ structure at $\chi_{BC}N = 200$ and $f_A = 0.5$, as presented in Figure 5. The plots are shown for those with $\chi_{AB/C}N = 80$ and $\chi_{AB/C}N = 190$, at which the hierarchical lamella with seven layers and nine layers are stable, respectively (see Figure 5a,b). When the $\chi_{AB/C}N$ increases, the density distribution for the outer layers becomes sharper but that for inner layers remains unchanged. This implies that the change in $\chi_{AB/C}N$ value only leads to the change in the interface between A domain and B domains. Therefore, if the hierarchical structure keeps unchanged, the increase in the $\chi_{AB/C}N$ is alleviated by reducing the interface between A and B blocks. However, when the $\chi_{AB/C}N$ becomes higher, the decrease in the A/B interface can no longer relieve the chain stretching in the outer layers, resulting in a frustrated structure. In this case, frustration is relieved by increasing the number of thin substructures because the A/B contact in such structures can be reduced significantly. This behavior can be further understood by examining the accumulative density. The results are given in Figure 5c where the integration of density along the arrow shown in Figure 5a,b is presented. The schematic lamellae are also provided to correspond to the accumulative density. The accumulative density in outer layers is reduced when the small-length-scale lamellae change from seven layers to nine layers, suggesting that the magnitude of A/B contact is effectively decreased by increasing the number of substructures. Consequently, the hierarchical structures have a preference for more substructures when the value of $\chi_{AB/C}N$ increases.

Some experimental results of hierarchically ordered structures are available in the literature for supporting our theoretical predictions. Matsushita et al. have investigated the double periodic structures self-assembled from multiblock terpolymers with the types of V(IS)$_n$IV and V(IS)$_n$I (V, I, and S are poly(2-vinylpyridine), polyisoprene, and polystyrene, respectively).[27−31] For these terpolymers, the lengths of I and S blocks are equal. In the observed double periodic hierarchical microstructures, the substructures having small periodicities are packed parallel to the structures possessing large periodicities. As the V volume fraction increases, the hierarchically ordered structures change from spheres-in-lamellae, to cylinders-in-lamellae, to lamellae-in-lamella, then to coaxial cylinder, and finally to onionlike sphere. This route of phase transition discovered in the experiments is in well accordance with the sequence shown in Figure 2: spheres-in-lamellae$^{\|}$ → cylinders-in-lamellae$^{\|}$ → lamellae-in-lamella$^{\|}$ → cylinders-in-cylinder$^{\|}$ → spheres-in-sphere$^{\|}$ transition as the volume fraction of A blocks increases.

Matsushita et al. also designed an new undecablock copolymer of S(IS)$_n$IS type by replacing the V blocks of V(IS)$_n$IV terpolymers with S blocks, where the two end S blocks are longer than the middle S blocks.[28,31,65] Both undecablock copolymers and terpolymers can form the hierarchical lamellar microstuctures. However, the number of thin lamellae within the large lamella is decreased from five to three when the molecular architecture is changed from V(IS)$_4$IV to S(IS)$_4$IS type. It is noted that, for S(IS)$_4$IS copolymer, the interactions between the end blocks and the middle blocks (i.e., the middle I or S) are weaker compared with the V(IS)$_4$IV terpolymers.[28,31] In our calculations, we found the number of thin substructures within large-length-scale structures is reduced when the interaction strength between the A end blocks and the repeating BC blocks is decreased, as shown in Figure 4. Our theoretical results are in excellent agreement with the experimental observations.

2. A(BC)$_n$ Multiblock Copolymers with $\chi_{AB}N > \chi_{AC}N$. In this section, the interaction strength $\chi_{AB}N$ was set to be greater than $\chi_{AC}N$. Under this condition, the A/C contact becomes more energetically favored relative to the A/B contact in terms of interaction enthalpy. Therefore, it is possible for the A/C interface to be formed, although there is no chain junction between A and C blocks.

When $\chi_{BC}N$ is smaller, the hierarchical microstructures exhibit a similar fully parallel version as shown in Figure 2. Interestingly, as $\chi_{BC}N$ is large enough, the hierarchical microstructures present a distinct microdomain organization where the two different-length-scale structures are arranged in perpendicular. Figure 6 shows the obtained perpendicular packed hierarchical structures of A(BC)$_3$ multiblock copolymers with $\chi_{BC}N = 600$. As can be seen from Figure 6a, when the value of f_A is 0.20, the multiblock copolymers self-assemble into hexagonally packed cylinders

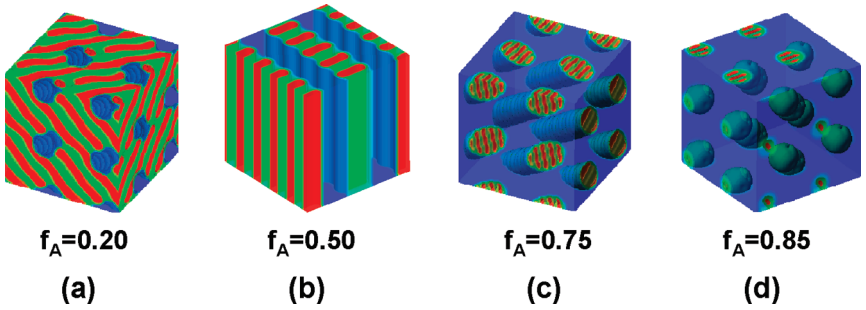

Figure 6. Hierarchical microstructures self-assembled from $A(BC)_3$ multiblock copolymer with $\chi_{BC}N = 600$: (a) cylinders-in-lamellae$^{\perp}$, (b) lamellae-in-lamella$^{\perp}$, (c) lamellae-in-cylinder$^{\perp}$, and (d) lamellae-in-sphere$^{\perp}$. From (a) to (d), the volume fractions of A blocks are 0.20, 0.50, 0.75, and 0.85, respectively. Other parameters for (a, b) are $\chi_{AB}N = 100$ and $\chi_{AC}N = 50$ and for (c, d) are $\chi_{AB}N = 150$ and $\chi_{AC}N = 100$. The blue, red, and green colors are assigned to A, B, and C blocks, respectively.

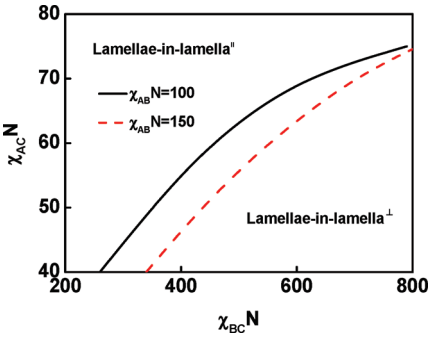

Figure 7. Phase diagram in $\chi_{AB}N-\chi_{BC}N$ space for the hierarchical lamellar structures of $A(BC)_3$ multiblock copolymers with $f_A = 0.5$. The solid and dashed lines are the phase boundaries for multiblock copolymers with $\chi_{AB}N = 100$ and $\chi_{AB}N = 150$, respectively.

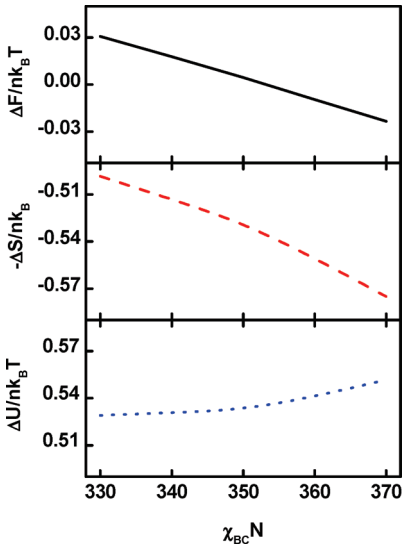

Figure 8. Free energy difference, conformational entropy difference, and enthalpy difference between the perpendicular and parallel packed lamellae-in-lamella structures as a function of $\chi_{BC}N$ for $A(BC)_3$ multiblock copolymers with $f_A = 0.5$, $\chi_{AB}N = 100$, and $\chi_{AC}N = 50$.

at large length scale. Within the matrix, the B and C blocks form a small-length-scale lamellar order of alternating B and C layers, which is arranged perpendicular to the axes of A cylinders. At $f_A = 0.50$ (Figure 6b), it can be seen that the B and C blocks form alternating layers within a large-length-scale lamella consisting of alternating A and BC layers. Figures 6c ($f_A = 0.75$) and 6d ($f_A = 0.85$) respectively show large-length-scale cylindrical and spherical morphologies whose cylinders and spheres are phase separated into small-length-scale alternating B and C layers. We define above microstructures respectively as cylinders-in-lamellae$^{\perp}$, lamellae-in-lamella$^{\perp}$, lamellae-in-cylinder$^{\perp}$, and lamellae-in-sphere$^{\perp}$. The prime symbol $\perp$ refers to the morphologies where hierarchical two length-scale-order structures are in perpendicular.

Notwithstanding the visual evidence of perpendicular packed structure-in-structures, there remains a concern as to under which condition these structures exist. From the calculation results, we learned that the perpendicular packed structure-in-structures are only stable at higher value of interaction strength $\chi_{BC}N$. This can be viewed from a phase diagram of the hierarchical lamellar structures, as illustrated in Figure 7. The phase diagram is in the space of $\chi_{AC}N$ vs $\chi_{BC}N$. The phase boundaries are determined by comparing the free energies of lamellae-in-lamella$^{\parallel}$ with five BCBCB layers and lamellae-in-lamella$^{\perp}$. As can be seen, the lamellae-in-lamella$^{\parallel}$ transform to lamellae-in-lamella$^{\perp}$ when the value of $\chi_{BC}N$ becomes greater. It is also noted that the phase boundary shifts toward higher value of $\chi_{BC}N$ as $\chi_{AC}N$ increases. Furthermore, the phase boundary shows a shift to higher $\chi_{BC}N$ value with increasing $\chi_{AB}N$. Such phase behavior could be generalized to other (parallel packed structure-in-structures) → (perpendicular packed structure-in-structures) phase transitions, although we do not map the other phase diagrams due to the huge computation cost.

To further understand the behavior that the perpendicular packed structure-in-structures are more stable than parallel packed structure-in-structures at higher $\chi_{BC}N$ value when $\chi_{AB}N > \chi_{AC}N$, we examined the free energy difference, enthalpy difference, and conformational entropy loss difference between perpendicular packed lamellae-in-lamella and parallel packed lamellae-in-lamella with five BCBCB layers. The results are presented in Figure 8. When the free energy difference becomes negative, the lamellae-in-lamella$^{\perp}$ is stable instead of lamellae-in-lamella$^{\parallel}$. Figure 8a shows the lamellae-in-lamella$^{\perp}$ is stable when $\chi_{BC}N$ is greater than 351 for multiblock copolymers with $\chi_{AB}N = 100$ and $\chi_{AC}N = 50$. In the calculated $\chi_{BC}N$ range, the entropy loss difference is always negative, while the enthalpy difference is positive, as can be seen from Figure 8b,c. This implies that in the lamellae-in-lamella$^{\perp}$ the loss of conformational entropy is smaller than that of lamellae-in-lamella$^{\parallel}$, but the interaction enthalpy is larger than that of lamellae-in-lamella$^{\parallel}$. As $\chi_{BC}N$ increases, the entropy loss difference shows a dramatic drop and the enthalpy difference slightly rises. Thus, at higher value of $\chi_{BC}N$, the lamellae-in-lamella$^{\perp}$ is energetically favorable due to dramatic reduce in loss of conformational entropy, although the enthalpy is unfavorable relative to the lamellae-in-lamella$^{\parallel}$. The increase in value of either $\chi_{AB}N$ or

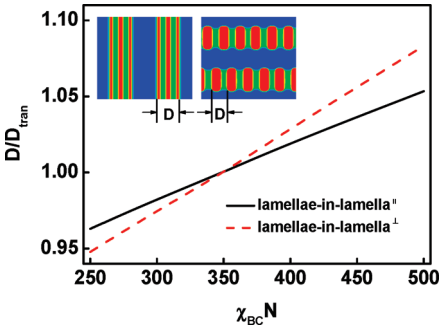

Figure 9. Relative lamellar spacing D/D_{tran} as a function of $\chi_{BC}N$ for perpendicular and parallel packed lamellae-in-lamella at $f_A = 0.5$. The D for each structure is schematically presented in the inset. D_{tran} is the equilibrium spacing at $\chi_{BC}N = 351$ where the phase transition takes place. Other interaction strengths are $\chi_{AB}N = 100$ and $\chi_{AC}N = 50$.

$\chi_{AC}N$ induces a great increase in interfacial energy of lamellae-in-lamella$^{\perp}$, leading to a shift of phase boundaries to higher $\chi_{BC}N$ as $\chi_{AB}N$ or $\chi_{AC}N$ increases. We can deduce that the reason why other perpendicular hierarchical structures are stable at higher value of $\chi_{BC}N$ is also the entropy driving.

Entropically the perpendicular packed structure-in-structure morphologies are optimal compared with the parallel hierarchical structures, as confirmed by Figure 8. The entropy of the multiblock copolymers includes two parts: molecular configuration and the chain stretching. Thus, the explanation that the entropy in perpendicular packed hierarchical structure is favorable can be due to two reasons. One reason is that the configuration number in perpendicular packed hierarchical structure is larger than that in parallel packed hierarchical structure. Taking the hierarchical lamellar structures of $A(BC)_3$ multiblock copolymer as an example, in the lamellae-in-lamella$^{\perp}$, the B and C end blocks adopt a fixed dangled conformation, while the remainder $(BC)_2$ midblocks assume configurations ranging from fully looping to fully bridging. However, in the lamellae-in-lamella$^{\parallel}$, the B and C blocks are confined to five BCBCB layers. As a result, the possible conformation number of B and C end blocks is as same as that in lamellae-in-lamella$^{\perp}$, but the conformation number of $(BC)_2$ midblocks decreases because the conformations such as full bridging conformation are excluded. The decrease in conformation number results in a reduction in conformational entropy.

Another reason is that, compared with the parallel packed hierarchical structures, the B and C chains in perpendicular packed hierarchical structures suffer from less marked confinement imposed by the large A layers because the substructures orient perpendicularly to the confined layers to retain bulk period. Direct evidence supporting this explanation was obtained by examining the period variation of microstructure. Figure 9 shows the relative period variation of lamellar phase as a function of $\chi_{BC}N$. The period D of each structure is illustrated in the inner of diagram. D is the lamellar spacing of substructures for lamellae-in-lamella$^{\perp}$ and the total period of small-length-scale structures for lamellae-in-lamella$^{\parallel}$, respectively. The D/D_{tran} is defined as relative period, where D_{tran} is the equilibrium period of each structures at $\chi_{BC}N = 351$ where the phase transition occurs. The D/D_{tran} is used to reflect the relative B and C chain stretching with respect to $\chi_{BC}N$. As shown in Figure 9, the relative period D/D_{tran} becomes larger as $\chi_{BC}N$ increases due to the increases in repulsion between B and C blocks. Compared with lamellae-in-lamella$^{\parallel}$, the D/D_{tran} of lamellae-in-lamella$^{\perp}$ is more sensitive to the change in value of $\chi_{BC}N$. The result suggests that the B and C chains in lamellae-in-lamella$^{\perp}$ are easier to be stretched relative to lamellae-in-lamella$^{\parallel}$. This is because, as the constraint is imposed by the A domains, the B and C chains in perpendicular packed hierarchical structures can be relaxed by reorienting the substructure along the unconfined directions in contrast to the parallel packed hierarchical structures. These two reasons result in a dramatic reduce in entropy loss in perpendicular hierarchical structure.

Recently, Bates et al. published an experimental observation of a lamellar structure containing the small-length-scale lamellae arranged perpendicular to the larger layered structures.[32,33] The hierarchical microstructure is self-assembled from a hexablock terpolymer consisting of equal volume fraction of P and compositional symmetric CECEC, where P, C, and E are poly(ethylene-*alt*-propylene), poly(cyclohexylethylene), and poly(ethylene), respectively. This complex morphology with two different length scales, which is related to the local (C−E) and overall (C−E−P) sequence, was obtained by microphase separation through chemical incompatibility between P, C, and E. It is established that the sequence of segment−segment interaction strength that governs P, C, and E blocks is as follow: $\chi_{CE} > \chi_{CP} > \chi_{EP}$. These experimental results are in good agreement with our theoretical results that the perpendicular packed structure-in-structure morphologies are formed at higher value of $\chi_{BC}N$ for $\chi_{AB}N > \chi_{AC}N$. From our results, we can rationalize the perpendicular arrangement of two-length-scale structures based on the segment−segment interaction parameter: $\chi_{BC}N > \chi_{AB}N > \chi_{AC}N$. Here, the A, B, and C blocks of $A(BC)_n$ multiblock copolymer correspond to the P, C, and E blocks of CECECP terpolymer molecule, respectively. More interestingly, we also observed other perpendicular packed microstructures such as lamellae-in-cylinder$^{\perp}$ and lamellae-in-sphere$^{\perp}$ when A volume fraction changes. We hope these novel morphologies could be observed in the future experimental studies.

In the present work, fascinating hierarchically ordered structures, including the parallel and perpendicular packed structure-in-structures, were observed for multiblock copolymer system with hierarchical competing interactions. These SCFT results are well consistent with the observations in experiments.[27−33] The SCFT simulations not only reproduce the experimental results but also provide guidance for further investigations. For instance, the perpendicular packed structure-in-structure morphologies such as lamellae-in-cylinder$^{\perp}$ and lamellae-in-sphere$^{\perp}$, which have not been observed in experiments, were expected in future studies. It is anticipated that the present work could be valuable for producing crucially fundamental and practical achievements, examples of which include design of functional nanostructured materials such as optical crystals,[18,21] development of materials with enhanced mechanical response,[33] and production of hierarchical organic/inorganic hybrid nanocomposites.[66]

Conclusion

We employed the real-space self-consistent field theory to explore the hierarchically ordered microstructures of $A(BC)_n$ multiblock copolymers. Parallel and perpendicular arranged hierarchical microstructures were found on the basis of two different types of relative interaction strength: one is that the interaction strength $\chi_{AB}N$ is less than or equal to $\chi_{AC}N$, and the other is that $\chi_{AB}N$ is greater than $\chi_{AC}N$. For the first case, only parallel packed structure-in-structures appear, such as cylinders-in-lamellae$^{\parallel}$, lamellae-in-lamella$^{\parallel}$, cylinders-in-cylinder$^{\parallel}$, and spheres-in-sphere$^{\parallel}$. These microstructures have different number of substructures depending on both the number n of repeating BC

blocks and interaction strength between A blocks and BC blocks. For the second case, the multiblock copolymers can form parallel packed structure-in-structure as well as perpendicular packed structure-in-structure morphologies. It was found that the perpendicular packed hierarchical morphologies are only stable at higher value of $\chi_{BC}N$. Our results are helpful for designing various packed hierarchical microstructures in complex copolymers.

Acknowledgment. This work was supported by National Natural Science Foundation of China (50925308). Support from projects of Shanghai municipality (09XD1401400, 0952 nm05100, 08DZ2230500, and B502) is also appreciated.

References and Notes

(1) Zvelindovsky, A. V. *Nanostructured Soft Matter: Experiment, Theory, Simulation and Perspectives*; Canopus Press: Bristol, UK, 2007.
(2) Hadjichristidis, N.; Pispas, S.; Floudas, G. A. *Block Copolymers: Synthetic Strategies, Physical Properties and Applications*; John Wiley & Sons: Hoboken, NJ, 2003.
(3) Bates, F. S. *Science* **1991**, *251*, 898–905.
(4) Hamley, I. W. *The Physics of Block Copolymers*; Oxford University Press: Oxford, UK, 1998.
(5) Lodge, T. P. *Macromol. Chem. Phys.* **2003**, *204*, 265–273.
(6) Bates, F. S.; Fredrickson, G. H. *Annu. Rev. Phys. Chem.* **1990**, *41*, 525–557.
(7) Bates, F. S.; Fredrickson, G. H. *Phys. Today* **1999**, *52*, 32–38.
(8) Tyler, C. A.; Morse, D. C. *Phys. Rev. Lett.* **2005**, *94*, 208302.
(9) Matsushita, Y.; Nomura, M.; Watanabe, J.; Mogi, Y.; Noda, I.; Imai, M. *Macromolecules* **1995**, *28*, 6007–6013.
(10) Matsen, M. W.; Thompson, R. B. *J. Chem. Phys.* **1999**, *111*, 7139–7146.
(11) Hermel, T. J.; Wu, L.; Hahn, S. F.; Lodge, T. P.; Bates, F. S. *Macromolecules* **2002**, *35*, 4685–4689.
(12) Wu, L.; Lodge, T. P.; Bates, F. S. *Macromolecules* **2004**, *37*, 8184–8187.
(13) Tyler, C. A.; Qin, J.; Bates, F. S.; Morse, D. C. *Macromolecules* **2007**, *40*, 4654–4668.
(14) Guo, Z.; Zhang, G.; Qiu, F.; Zhang, D.; Yang, Y.; Shi, A.-C. *Phys. Rev. Lett.* **2008**, *101*, 028301.
(15) Yamauchi, K.; Akasaka, S.; Hasegawa, H.; Iatrou, H.; Hadjichristidis, N. *Macromolecules* **2005**, *38*, 8022–8027.
(16) Hanski, S.; Houbenov, N.; Ruokolainen, J.; Chondronicola, D.; Iatrou, H.; Hadjichristidis, N.; Ikkala, O. *Biomacromolecules* **2006**, *7*, 3379–3384.
(17) Goldacker, T.; Abetz, V.; Stadler, R.; Erukhimovich, L.; Leibler, L. *Nature* (*London*) **1999**, *398*, 137–139.
(18) Erukhimovich, I.; Smirnova, Y. G.; Abetz, V. *J. Polym. Sci., Ser. A* **2005**, *45*, 1093–1105.
(19) Ikkala, O.; ten Brinke, G. *Science* **2002**, *295*, 2407–2409.
(20) Ruokolainen, J.; Makinen, R.; Torkkeli, M.; Makela, T.; Serimaa, R.; ten Brinke, G.; Ikkala, O. *Science* **1998**, *280*, 557–560.
(21) Valkama, S.; Kosonen, H.; Ruokolainen, J.; Haatainen, T.; Torkkeli, M.; Serimaa, R.; ten Brinke, G.; Ikkala, O. *Nat. Mater.* **2004**, *3*, 872–876.
(22) Ruokolainen, J.; ten Brinke, G.; Ikkala, O. *Adv. Mater.* **1999**, *11*, 777–780.
(23) Ruotsalainen, T.; Turku, J.; Heikkila, P.; Ruokolainen, J.; Nykanen, A.; Laitinen, T.; Torkkeli, M.; Serimaa, R.; ten Brinke, G.; Harlin, A.; Ikkala, O. *Adv. Mater.* **2005**, *17*, 1048–1052.
(24) Tung, S.-H.; Kalarickal, N. C.; Mays, J. W.; Xu, T. *Macromolecules* **2008**, *41*, 6453–6462.
(25) Nandan, B.; Lee, C. H.; Chen, H. L.; Chen, W. C. *Macromolecules* **2005**, *38*, 10117–10126.
(26) Ansari, I. A.; Castelletto, V.; Mykhaylyk, T.; Hamley, I. W.; Lu, Z. B.; Itoh, T.; Imrie, C. T. *Macromolecules* **2003**, *36*, 8898–8901.
(27) Matsushita, Y. *Polym. J.* **2008**, *40*, 177–183.
(28) Matsushita, Y.; Takano, A.; Hayashida, K.; Asari, T.; Noro, A. *Polymer* **2009**, *50*, 2191–2203.
(29) Matsushita, Y. *Macromolecules* **2007**, *40*, 771–776.
(30) Masuda, J.; Takano, A.; Suzuki, J.; Nagata, Y.; Noro, A.; Hayashida, K.; Matsushita, Y. *Macromolecules* **2007**, *40*, 4023–4027.
(31) Masuda, J.; Takano, A.; Nagata, Y.; Noro, A.; Matsushita, Y. *Phys. Rev. Lett.* **2006**, *97*, 098301.
(32) Fleury, G.; Bates, F. S. *Macromolecules* **2009**, *42*, 1691–1694.
(33) Fleury, G.; Bates, F. S. *Macromolecules* **2009**, *42*, 3598–3610.
(34) Kriskin, Y. A.; Erukhimovich, I. Y.; Khalatur, P. G.; Smirnova, Y. G.; ten Brinke, G. *J. Chem. Phys.* **2008**, *128*, 244903.
(35) Subbotin, A.; Klymko, T.; ten Brinke, G. *Macromolecules* **2007**, *40*, 2915–2918.
(36) Klymko, T.; Subbotin, A.; ten Brinke, G. *J. Chem. Phys.* **2008**, *129*, 114902.
(37) Klymko, T.; Markov, V.; Subbotin, A.; ten Brinke, G. *Soft Matter* **2009**, *5*, 98–103.
(38) Nap, R.; Sushko, N.; Erukhimovich, I.; ten Brinke, G. *Macromolecules* **2006**, *39*, 6765–6770.
(39) Li, W.; Shi, A.-C. *Macromolecules* **2009**, *42*, 811–819.
(40) Fredrickson, G. H. *The Equilibrium Theory of Inhomogeneous Polymers*; Oxford University Press: Oxford, UK, 2006.
(41) Drolet, F.; Fredrickson, G. H. *Phys. Rev. Lett.* **1999**, *83*, 4317–4320.
(42) Ganesan, V.; Fredrickson, G. H. *Europhys. Lett.* **2001**, *55*, 814–820.
(43) Drolet, F.; Fredrickson, G. H. *Macromolecules* **2001**, *34*, 5317–5324.
(44) Matsen, M. W. *J. Phys.: Condens. Matter* **2002**, *14*, R21–R47.
(45) Matsen, M. W.; Thompsom, R. B. *J. Chem. Phys.* **1999**, *111*, 7139–7146.
(46) Matsen, M. W.; Schick, M. *Phys. Rev. Lett.* **1994**, *72*, 2660–2663.
(47) Lee, J. Y.; Thompson, R. B.; Jasnow, D.; Balazs, A. C. *Macromolecules* **2002**, *35*, 4855–4858.
(48) Thompson, R. B.; Ginzburg, V. V.; Matsen, M. W.; Balazs, A. C. *Macromolecules* **2002**, *35*, 1060–1071.
(49) Wang, R.; Li, W.; Luo, Y.; Li, B.; Shi, A.-C.; Zhu, S. *Macromolecules* **2009**, *42*, 2275–2285.
(50) Jiang, R.; Jin, Q.; Li, B.; Ding, D.; Wickham, R. A.; Shi, A.-C. *Macromolecules* **2008**, *41*, 5457–5465.
(51) Wang, L.; Zhang, L.; Lin, J. *J. Chem. Phys.* **2008**, *129*, 114905.
(52) Jiang, Z.; Wang, R.; Xue, G. *J. Phys. Chem. B* **2009**, *113*, 7462–7467.
(53) Ye, X.; Shi, T.; Lu, Z.; Zhang, C.; Sun, Z.; An, L. *Macromolecules* **2005**, *38*, 8853–8857.
(54) Chen, P.; Liang, H.; Shi, A.-C. *Macromolecules* **2008**, *41*, 8938–8943.
(55) Zhang, L.; Lin, J.; Lin, S. *J. Phys. Chem. B* **2008**, *112*, 9720–9728.
(56) Zhang, L.; Lin, J.; Lin, S. *Macromolecules* **2007**, *40*, 5582–5592.
(57) Zhang, L.; Lin, J.; Lin, S. *Soft Matter* **2009**, *5*, 173–181.
(58) Cochran, E. W.; Garcia-Cervera, C. J.; Fredrickson, G. H. *Macromolecules* **2006**, *39*, 2449–2451.
(59) Wang, L.; Lin, J.; Zhang, L. *Langmuir* **2009**, *25*, 4725–4742.
(60) Matsen, M. W.; Bates, F. S. *J. Chem. Phys.* **1997**, *106*, 2436–2448.
(61) Lennon, E. M.; Mohler, G. O.; Ceniceros, H. D.; Garcia-Cervera, C. J.; Fredrickson, G. H. *Multiscale Model. Simul.* **2008**, *6*, 1347–1370.
(62) Eyert, V. *J. Comput. Phys.* **1996**, *124*, 271–285.
(63) Bohbot-Raviv, Y.; Wang, Z.-G. *Phys. Rev. Lett.* **2000**, *85*, 3428–3431.
(64) Sun, M.; Wang, P.; Qiu, F.; Tang, P.; Zhang, H.; Yang, Y. *Phys. Rev. E* **2008**, *77*, 016701.
(65) Nagata, Y.; Masuda, J.; Noro, A.; Cho, D.; Takano, A.; Matsushita, Y. *Macromolecules* **2005**, *38*, 10220–10225.
(66) Zhang, L.; Lin, J. *Macromolecules* **2009**, *42*, 1410–1414.